Ol.A. Savchuk, J.J. Carvajal,, J. Massons, C. Cascales, M. Aguiló, F. Díaz. Sensors and Actuators A 250 (2016) 87–95*

Novel low-cost, compact and fast signal processing sensor for ratiometric luminescent nanothermometry

Ol.A. Savchuk,[1] J.J. Carvajal,[1,*] J. Massons,[1] C. Cascales,[2] M. Aguiló,[1] F. Díaz[1]

[1]*Física i Cristal·lografia de Materials i Nanomaterials (FiCMA-FiCNA) and EMaS, Universitat Rovira i Virgili (URV), c/Marcel·lí Domingo 1, E-43007, Tarragona, Spain*

[2]*Instituto de Ciencia de Materiales de Madrid, c/ Sor Juana Inés de la Cruz, Cantoblanco, Madrid, 28049, Spain*

*Corresponding author: joanjosep.carvajal@urv.cat

Keywords: temperature sensor, non-invasive, luminescence, up-conversion, nanoparticles.

Abstract

We developed a new compact, low-cost and non-invasive temperature sensor based on a ratiometric luminescence technique. The setup included a commercial digital color sensor, which collects simultaneously signals in the blue, green and red regions of the electromagnetic spectrum, usually used to assess the quality of computer screens and used for the first time here as a sensor for luminescent thermometry, coupled to an optical system that focuses an excitation laser beam onto luminescent nanoparticles emitting at least in two of these electromagnetic regions, which simplifies considerably the design, alignment and measurement procedures of setups used up to now for the same purpose. The same optical system collects the emission arising from the luminescent nanoparticles and directs it towards the digital color sensor through a dichroic mirror. We probed the potentiality of this setup for luminescence thermometry in the biological range of temperatures using Er,Yb:$NaYF_4$, and up to 673 K for microelectronic applications using Tm,Yb:$GdVO_4$ up-converting nanoparticles. The thermal sensitivity obtained in both cases is similar to that previously reported for the same kinds of nanoparticles using conventional systems. This validates our setup for temperature measurements. Also, we developed new flexible and transparent polymer composites, in which we embedded upconversion luminescent nanoparticles of Er,Yb:$NaYF_4$ in PDMS, a standard polymer for microfluidic devices used for biomedical studies, which allow fabricating thermometric microfluidic chips in which temperature can be determined using our setup. The thermal sensitivity for these composites is slightly smaller than that of the bare nanoparticles, bur still allowing for precise and fast temperature measurements.

1. Introduction

There are many areas of industry, where temperature measurements are essential, such as metallurgical industries, glass manufacturing, material modeling or dairy products, among others. There are other fields like biomedical sciences, where temperature provides basic diagnostic criteria [1, 2] and its control is essential during hyperthermia treatments [3, 4], for instance. Despite modern temperature measurement instruments at the nanoscale are in general complex in nature and at the same time fascinating in operation [5], there are situations -because of hostile environments, presence of vibrations, electrical noise, strong electromagnetic fields, or other factors- where temperature measurements are difficult or even impossible with this kind of instruments. To overcome these difficulties and achieve temperature sensing in hardly accessible locations, optical non-contact thermometry methods have been developed since they provide electromagnetic immunity and possibilities for remote measurements [6, 7]. Most of the optical non-contact temperature sensors are based on reflection, absorption, scattering, fluorescence or interference phenomena of light [8, 9]. Among these optical non-contact thermometry methods, fluorescence thermometry is among the most versatile methods. It is based on fluorescence intensity, band-shift or lifetime changes produced by temperature [10]. Among these three techniques, it is difficult to select the optimal one, as each of them shows special features of interest. The lifetime-based technique allows performing measurements in objects in movement and at high temperature, for instance, avoiding the blackbody radiation effect [10, 11]. However, this technique requires costly instrumentation, such as pulsed lasers for excitation of the luminescent probe, and monochromators to isolate the particular wavelength to be analyzed, and in some cases lock-in amplifiers to be able to measure small intensity signals. From another side, the band-shift technique can be very sensitive to temperature changes, but it can be only applied to a relatively narrow range of temperatures. Furthermore, since this technique has mainly used quantum dots a luminescent nanoparticles, it suffers from their signal bleaching. By using ratiometric measurements these problems can be avoided [6, 7]. Ratiometric measurements are based on systems with different luminescence emission bands whose relative intensities strongly depend on temperature. This thermal dependency is caused by a thermally induced electronic population re-distribution among the corresponding emitting energy levels of the optical center. An additional advantage is that the relative intensity of the luminescence bands depends only on temperature but not on the local concentration of the emitting center. Also, effects derived from fluctuations in the excitation source are avoided since the different luminescence lines will be affected in an equal manner.

In these techniques, the choice of a particular luminescent material determines the temperature range, thermal sensitivity and stability of the nanothermometer. The most used materials for luminescent nanothermometry are quantum dots [12-14], organic dyes [15-17] and lanthanide-doped materials [18-21]. Although, organic dyes and quantum dots show a high thermal sensitivity, their main disadvantage is that they need to be excited using ultraviolet (UV) or visible light (although recently quantum dots have been developed that can be excited in the near-infrared that can overcome this problem, see for instance [22]). This may lead to the degradation of the fluorescent material. Furthermore, when used in biological applications, the excitation with UV or visible light might induce the appearance of background fluorescence, and even the damage of biological tissues. From another side, the use of lanthanide-doped up-converting nanoparticles (Ln-UCNPs), which absorb photons sequentially in the near-infrared (NIR) and emit radiation in the visible, has several advantages, such as the negligible photodamage to living organisms, a weak autofluorescence background, and a deeper penetration in biological tissues for biomedical thermometry purposes. Moreover, NIR excitation can be achieved with high power, and low cost laser sources. Finally, it is also important to note that Ln-UCNPs are more optically stable and have lower toxicity than quantum dots, for instance.

However, the setups used up to now to determine changes in luminescence intensity with temperature in these ratiometric techniques require bulky and relatively costly equipment, such as monochromators, luminescence detectors (photomultiplier tubes, CCD cameras, etc.), lock-in amplifiers, oscilloscopes, sophisticated aligning mechanical systems, etc. The size of these devices also limits the practical applications of these thermometric techniques and their transfer to real industrial or medical environments, where the measurement conditions change continuously. Furthermore, recording an emission spectrum with these devices requires some seconds, or even minutes, a timeframe during which the temperature of the sample might change, which represents an additional disadvantage of this technology.

Here, we report a new low-cost, compact, fast signal processing, and non-invasive temperature sensor using a ratiometric fluorescence thermometry technique that simplifies substantially the design, alignment and measurement procedures of setups used previously for the same purpose. Our setup uses a commercial digital color sensor, usually used to assess the quality of computer screens and used here for the first time to undertake luminescence thermometric measurements, coupled to an optical system that allows simultaneously the excitation of the Ln-UCNPs and the collection of their emission, simplifying the alignment of the optical components (excitation sources, lenses, mirrors and detectors) of the measurement setup. The emission from the Ln-UCNPs is separated from the excitation radiation, and diverted towards the detector. The detector is build in a mosaic structure, and containing different filters that allows it detecting simultaneously signals in the red, green and blue channels. With a microprocessor we calculated the fluorescence intensity ratio corresponding to the signals of two of these channels, and

after comparing it to a previously determined calibration curve, temperature is visualized in a LCD display [23]. This reduces substantially the measurement procedures, times and processing of the luminescent signals used to determine the temperature. We used different Ln-UCNPs to demonstrate the potentiality of this thermometer to operate in different temperature ranges. We also reported, for the first time, the fabrication of transparent polydimethylsiloxane (PDMS)/luminescent Ln-UCNPs composites, from which microfluidic microchips can be fabricated since PDMS is one of most used polymers for this purpose [24,25]. These composites would allow to determine temperature directly in the internal walls of the microchips, taking into account that the fluid should be pumped to the wall of the microchannel so that as being in contact the fluid and the composite, the temperature determined might be representative of the temperature of the fluid, avoiding in this way that the fluid had to carry the luminescent thermometric material. This would simplify the fabrication and performance of similar systems reported previously involving the use of surface plasmons [26].

2. Experimental section

2.1 Temperature measurements setup

The setup we propose for temperature measurements comprises a diode laser that can be adapted to emitting at a wavelength that can be absorbed by the Ln-UCNPs, a focusing system (a microscope objective in the particular applications we are showing here, but that can be substituted easily by an optical lens) to focus the laser beam onto the sample and, that at the same time, collects the light emitted by the nanoparticles, a dichroic mirror that deviates the visible light generated by the nanoparticles towards the digital color sensor and at the same time filters the excitation radiation, and a S9706 Hamamatsu digital color sensor. A schematic representation of this setup is shown in Figure 1(a). The S9706 Hamamatsu digital color sensor consists on 9×9 arrayed photodiode elements arranged in a mosaic pattern integrated on a chip (see Figure 1(b)) with a photosensitive area of 1.2 × 1.2 mm. Each element has an on-chip filter that is sensitive to a particular range of wavelengths corresponding to different colors: red (590-720 nm), green (480-600 nm) and blue (400-540 nm), as shown in Figure 1(c). This sensor allows the RGB components of the incident light to be simultaneously measured with high accuracy. This digital color sensor is connected to a microchip that converts and amplifies the light signals into 12-bit digital signals, with independent reading for the blue, green and red channels, which allows us to analyze the intensity ratios between these signals, and to compare these data with a previous calibration curve to determine the temperature of a particular measurement. The integration time of this kind of sensor depends on the illuminance conditions, ranging from 100 s for low illuminance conditions to 10 μs for high illuminance conditions [27].

To establish the calibration curve, the Ln-UCNPs were introduced in a Linkam THMS 600 heating stage, taking measurements every 5 ºC when we analyzed the biological range of temperatures (25-60 ºC) and every 50 ºC for higher temperature applications. An Apollo Instruments Inc. diode laser with emission at 980 nm and 100 mW was used as the excitation source. The laser beam was focused on the sample using a 40X microscope objective and a N.A. of 0.6, producing a laser spot ~10 µm on the sample. The emission was collected by the same microscope objective, and after passing a dichroic filter for elimination of the excitation wavelength, was sent to the Hamamatsu S9706 sensor.

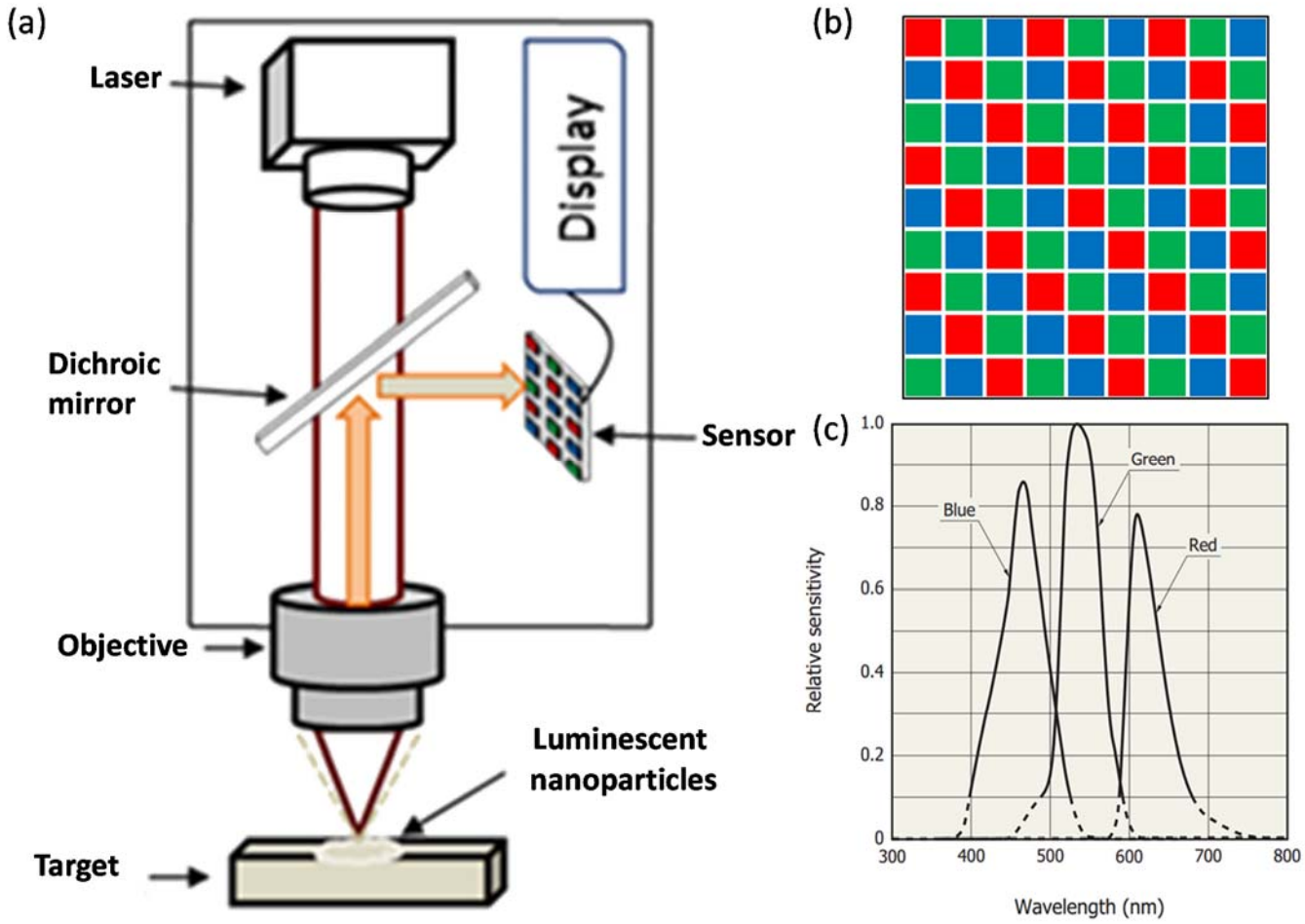

Figure 1. (a) Scheme of the temperature sensor we propose to use. (b) Structure of the Hamamatsu S9706 digital color sensor. (c) Relative sensitivity curve of the on-chip filters of the digital color sensor.

2.2 Ln-UCNPs synthesis and characterization

To demonstrate the operation of the sensor, we used different kinds of nanoparticles, with the only requirement that they emit light in two of the different ranges of the visible spectrum that can be detected by the Hamamatsu S9706 digital color sensor. An additional requirement we introduced was that the

particles could be excited in the NIR, so we used Ln-UCNPs, given their previously indicated advantages as well as the possibility of providing simultaneous imaging and temperature sensing at nanoscale [21]. We selected different Ln-UCNPs to show the potentiality of our setup to be used in different temperature ranges.

Hexagonal β-Er,Yb:$NaYF_4$ nanoparticles, with dopant concentrations of 2 mol% Er and 20 mol% Yb, and that have been extensively used to determine the temperature by optical methods in the biological range of temperatures [28], were provided by Boston Applied Technologies, Inc. From another side, we also used hydrothermally prepared Tm,Yb:$GdVO_4$@SiO_2 core-shell nanoparticles [29], with dopant concentrations of 1 mol% Tm and 15 mol% Yb, and which allow temperature determination up to 673 K with high sensitivity [30], and that can be used in microelectronics, for instance, to detect hot spots in microcircuits.

We recorded the emission spectra generated by the Ln-UCNPs by focusing the 980 nm diode laser beam through a 40X magnification microscope objective onto the sample, collecting the emission arising from the sample by the same objective, and sending the signal to an AVANTES AVS-USB 2000 fiberoptic spectrometer that recorded it.

2.3 Preparation and characterization of Ln-UCNPs embedded PDMS composites

To prepare Er,Yb:$NaYF_4$/PDMS composites, the silicon elastomer was firstly mixed with the curing agent, followed by ultrasonication at room temperature for 10 min. Then, different quantities of Er,Yb:$NaYF_4$ nanoparticles were added to the above mixture under mechanical stirring for 30 min at room temperature. In order to remove the bubbles formed after the mechanical stirring, the composite was placed in a desiccator for 1 h. Finally, the Er,Yb:$NaYF_4$/PDMS composite was placed in an oven at 353 K during 40 min for polymerization.

The emission spectra of these composites were collected as described in the previous section. Images of these luminescent composites were recorded with a charge coupled device (CCD) Thorlabs camera to determine the distribution of Ln-UCNPs in the silicone.

3. Results and discussion

3.1 Luminescent thermometry with Ln-UCNPs

The potentiality of our setup was demonstrated by using two different kinds of Ln-UCNPs, Er^{3+}-doped β-$NaYF_4$ and Tm^{3+}-doped $GdVO_4$, both of them sensitized with Yb^{3+}, which provide emission lines that overlap with the sensitivity curves of the on-chip filters of the digital color sensor in two different ways. Both kind of nanoparticles where excited at 980 nm, coinciding with the absorption band associated to the $^2F_{7/2} \rightarrow {}^2F_{5/2}$ transition of Yb^{3+}, that transfers its energy in a very efficient way to Er^{3+}

and Tm^{3+} [31]. Yb^{3+} was used as the sensitizer since its absorption cross-section at 980 nm is higher than that of Er^{3+} or Tm^{3+} at the same wavelength, allowing for a more brilliant emission from these ions [31]. Figure 2 shows the emission spectra of Er,Yb:$NaYF_4$ and Tm,Yb:$GdVO_4$ UCNPs after excitation at 980 nm, and the overlap with the detection ranges of the digital color sensor. In the case of Er,Yb:$NaYF_4$ nanoparticles the emission bands are located in the green and red regions of the electromagnetic spectrum, corresponding to the $^2H_{11/2}$, $^4S_{3/2} \rightarrow {}^4I_{15/2}$ and $^4F_{9/2} \rightarrow {}^4I_{15/2}$ transitions of Er^{3+}. In the case of Tm,Yb:$GdVO_4$ UCNPs the emission bands are located in the blue and red, corresponding to the $^1G_4 \rightarrow {}^3H_6$ and $^3F_3 \rightarrow {}^3H_6$ transitions of Tm^{3+}, that provide another example to calibrate the temperature by changes in the luminescence intensities.

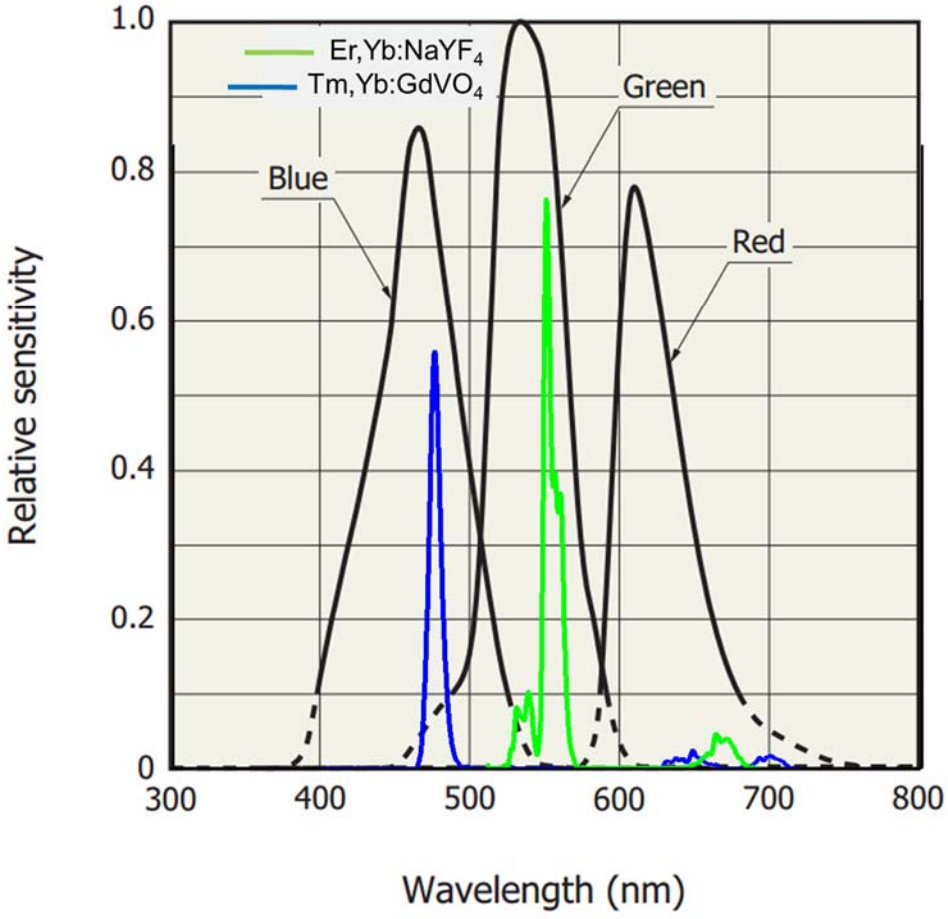

Figure 2. Overlap of the emission spectrum of Er,Yb:$NaYF_4$ and Tm,Yb:$GdVO_4$UCNPs with the detection ranges of the digital color sensor. Adapted from Digital Color Sensor S9706 datasheet, Hamamatsu.

Despite we cannot consider that the electronic levels from which the green and red emissions in the case of Er,Yb:$NaYF_4$ UCNPs, or the blue and red emissions in the case of Tm,Yb:$GdVO_4$ UCNPs are thermally coupled, since the electronic energy levels from which they arise lie too far apart, we observed that the intensity of these emission lines follows different tendencies as the temperature increased, as can be seen in Figures 3(a) and (b). As can be seen, in the case of Er,Yb:$NaYF_4$ nanoparticles (Figure 3(a)),

the intensity of the green band decreases slightly when the temperature increases, while the intensity of the red band increases slightly. The same trend can be observed even magnified Tm,Yb:$GdVO_4$ nanoparticles: the intensity of the blue emission drops substantially when the temperature increases, while the intensity of the red band increases substantially. Thus, although we cannot consider that these systems are in thermal equilibrium governed by a Boltzmann distribution, we can observe how the intensity ratio between these two groups of lines evolves with temperature, since at the end, the two electronic levels from which each group of emissions are generated, are electronically linked. In fact, the evolution of the intensity ratio calculated from the values obtained for the integration of the green and red, and blue and red channels, respectively, of the digital color sensor with temperature for the two kinds of nanoparticles is also presented in Figure 3, in the biological range of temperatures for Er,Yb:$NaYF_4$ UCNPs (see Figure 3 (c)), and in the range from room temperature to 673 K for Tm,Yb:$GdVO_4$ UCNPs (see Figure 3 (d)). It can be seen that the intensity ratio integrated from the two different channels in the case of Er,Yb:$NaYF_4$ nanoparticles follows almost a linear dependence, while in the case of Tm,Yb:$GdVO_4$ nanoparticles it follows an exponential dependence. The dispersion in the intensity ratios determined from the measurements performed with the digital color sensor is small and does not interfere in the determination of temperature, as can be seen in the figure. The fitting of the experimental points was done using an exponential equation of the form:

$$CT \qquad (1)$$

with the following parameters: A = 0.16, B = 0.16 and C = 0.0056 for for Er,Yb:$NaYF_4$ UCNPs, and A' = 0.23, B' = 0.38 and C' = 0.0024 for Tm,Yb:$GdVO_4$ UCNPs.

If we compare the evolution of the intensity ratios obtained for these nanoparticles using the digital sensor with that computed directly from the spectra shown in Figures 3 (a) and (b) (see Figure S1 in Supplementary Information), we observe that for Er,Yb:$NaYF_4$ nanoparticles the behavior is very similar. However, in the case of Tm,Yb:$GdVO_4$ nanoparticles we observe important differences, especially at high temperatures. This might be due to the sum of two effects, from one side, to the fact that the intensity of the blue emission is decreasing substantially at high temperatures, from the other, the emission in the deep red obtained with these nanoparticles does not match to the maximum sensitivity of the red channel of the digital sensor. Thus, in consequence, the accuracy of the measurements is not the optimal one. However, we have to keep in mind that we are comparing the measurements obtained with two systems with substantially different prices. The spectra were recorded with a fiberoptic spectrometer with a cost that in at least three orders of magnitude higher than that of the digital sensor, but it is important to note that when the intensity of the signals is the appropriate and the luminescence bands matches the maximum sensitivity of the detection channels of the digital sensor, both methods provide

similar results, allowing to decrease substantially the price of the detection scheme for luminescence thermometry.

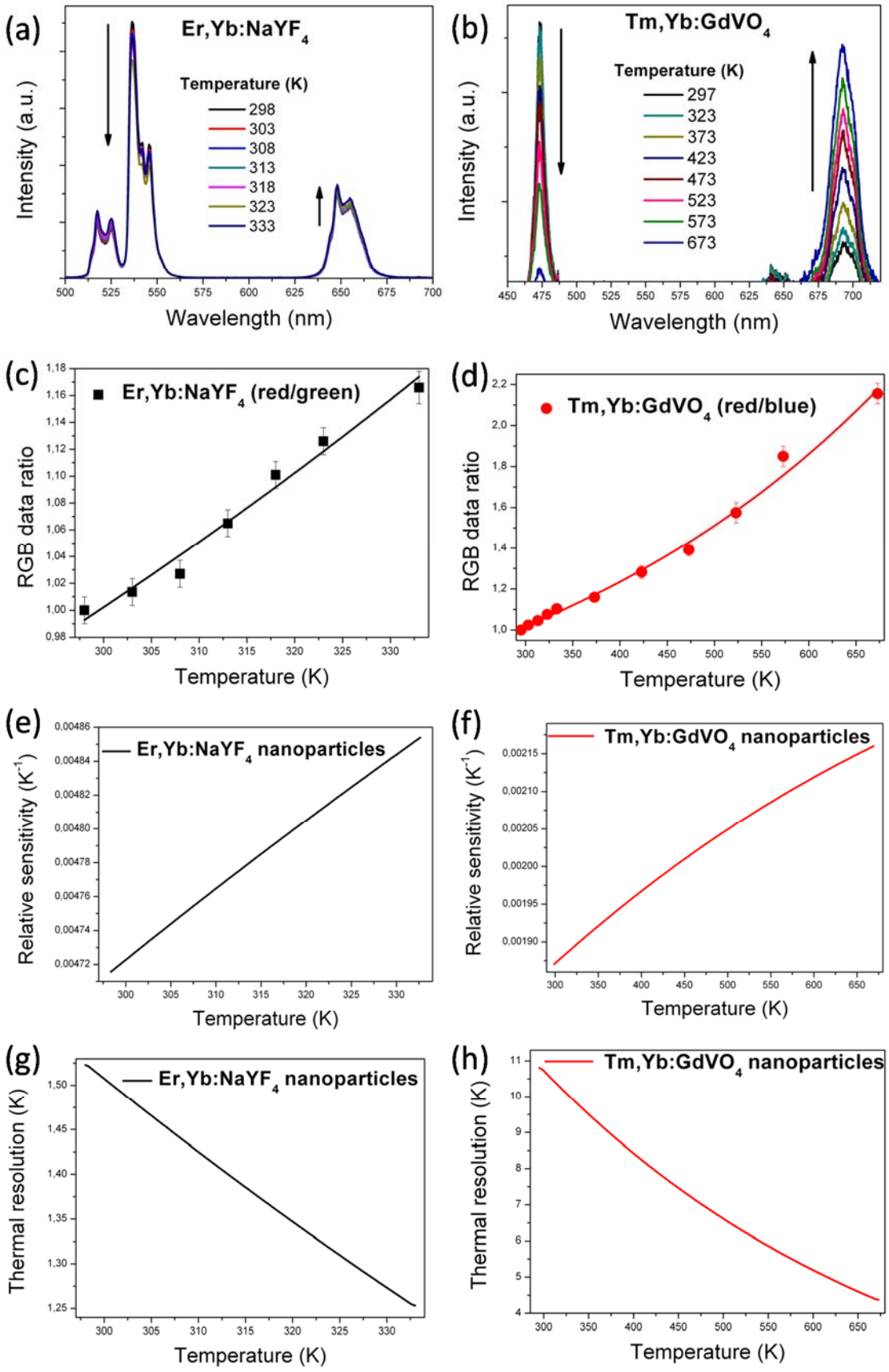

Figure 3. Evolution of the emission spectra with temperature for the (a) Er,Yb:$NaYF_4$ and (b) Tm,Yb:$GdVO_4$ nanoparticles. Evolution of the ratio between the signals of the blue, green and red channels recorded by the sensor with temperature for the (c) Er,Yb:$NaYF_4$ and (d) Tm,Yb:$GdVO_4$ nanoparticles. Relative thermal sensitivity for (e) Er,Yb:$NaYF_4$ and (f) Tm,Yb:$GdVO_4$ nanoparticles. Thermal resolution for the (g) Er,Yb:$NaYF_4$ and (h) Tm,Yb:$GdVO_4$ nanoparticles.

In order to compare the capacity for temperature determination of our sensor with that of other systems reported in the literature, we calculated the relative thermal sensitivity through the following equation [6]:

□□□□□= 1□□□ □□□□ □□□□□·□□□□ □□□□ □□□□□□□ (2)

The maximum relative thermal sensitivity for Er,Yb:$NaYF_4$ and Tm,Yb:$GdVO_4$UCNPs was found to be 0.5 and 0.2 % K^{-1}, respectively. The sensitivity value reported here for Tm,Yb:$GdVO_4$ nanoparticles, although smaller than that reported previously using a conventional system (1.54 % K^{-1}) [30], is similar to the one reported for other up-converting nanoparticles used for luminescence thermometry [32-34]. In the case of Er,Yb:$NaYF_4$ nanoparticles the relative thermal sensitivity reported in the literature varies from 0.21 to 1.24 % K^{-1} [20,35]. Thus, the relative thermal sensitivity value we obtained lies in this range of sensitivities, indicating that we can use our system, avoiding using expensive and bulky equipment.

) can be estimated as [36]:

1□□□·□□□□□□□□(□) (3)

is the standard deviation of the residuals in the fitting of the experimental points. Figures 3 (e) and (f) show the evolution of the thermal resolution of both kinds of nanoparticles as a function of temperature calculated using eq. 3. The better thermal resolution was obtained at high temperature in both cases. Er,Yb:$NaYF_4$ nanoparticles show a thermal resolution of around 1.52 K at room temperature that decreases as the temperature increases to a value of 1.25 K at 332 K, . Since the thermal resolution has not been reported for these nanoparticles using a conventional system, we cannot extract any conclusion about the influence of our system in this parameter. In the case of Tm,Yb:$GdVO_4$ nanoparticles, despite showing a higher thermal resolution, between 4 - 11 K, being the lowest value that corresponding to high temperature (675 K). These values are still valid to detect hot spots in microelectronic applications, for instance. In the case of the Er,Yb:$NaYF_4$ nanoparticles, the experimental points could also be fitted to a linear function (see Figure S2 in Supplementary Information). Nevertheless, the degree of improvement of the relative thermal sensitivity and the thermal resolution was very small when compared to the exponential fitting, from 0.48 % K^{-1} to 0.52 % K^{-1} in the case of the relative thermal sensitivity, and from 1.25 to 1.15 K in the case of the thermal resolution. Thus, although it does not exist un underlying theory that can support the use of an exponential function for the empirical fitting of the RGB data ratio, we decided to use it for both king of nanoparticles to have a uniformity in the treatment of the data in this manuscript.

3.2 Luminescent thermometry in polymer composites for microfluidics applications

Microfluidics systems offer several advantages in many aspects of analytical chemistry and biochemistry, including efficiency, speed, portability, and reduced amount of reagent consumption [37]. However, the accurate and precise temperature control inside a microfluidic system is crucial, and has been demonstrated in a variety of applications [38-40]. When thermometry contact methods have been used for this purpose, problems associated to the size probe that these devices present arised [41]. Alternatively, non-contact methods for temperature determination in microfluidics have been reported, including thermo-reflectance methods [42], Raman spectroscopy [43], nuclear magnetic resonance [44], or luminescent thermometry by mixing organic dyes with the fluid circuiting in the microchip [45]. However, both Raman spectroscopy and nuclear magnetic resonance are based on the measurements of properties of water molecules, so they can only be used for aqueous solutions. In the case of thermo-reflectance methods, despite they offer a high thermal and spatial resolution, the use of expensive and complicated equipment is needed. Finally, in the cases where luminescence thermometry has been used, the organic dyes included are usually toxic, furthermore, they should be soluble or miscible with the fluid circulating through the microchip, which also limit their range of applications in microfluidics. Additionally, if the fluorescent dye is mixed with the fluid, it gives only information about the fluid and not about the platform on which the microfluidics chip is fabricated. Thus, there is a need to develop a cheap and accurate temperature determination technique in microfluidic systems that can be integrated in the same microfluidic chip.

PDMS is one of the most common silicon-based polymers used in microfluidics, exhibiting a high flexibility, a high optical transparency, a low surface tension, a high hydrophobicity, high thermal and chemical resistances, and biocompatibility [46-48]. Because of its excellent properties this material has been used in a wide range of applications including the fabrication of microfluidic devices by soft-lithography systems [24], among others, and becoming one of the most popular polymers for lab-on-a-chip devices [25]. By generating organic / inorganic composites with this polymer, its properties have been complemented with additional ones introduced by the inorganic compounds. For instance, Fang and co-workers embedded Au nanocrystals in PDMS to generate plasmonic heating in a single device for microfluidic applications [49]. The mixing of magnetic nanoparticles with PDMS allowed producing magnetic and conductive composites for biological sensing purposes [50]. Also, by mixing luminescence nanoparticles with PDMS an enhanced luminescence has been reported [51].

Inspired by these works, we prepared Er,Yb:$NaYF_4$/PDMS composites as a new material that allows the fabrication of microfluidic chips for biological applications and at the same time allows

temperature determination, namely thermal sensing on the surface and the internal part of a microfluidic chip based on our composite, through a non-contact and non-invasive method. Furthermore, by combining it with the experimental setup we designed, it might allow for the temperature determination in a compact device, perfect for the miniaturization of the whole system, and avoiding the use of bulk equipment for the same purpose.

Figure 4(a) depicts photographs of the Er,Yb:$NaYF_4$/PDMS composites containing different concentrations of luminescent nanoparticles. In the images, the optical transparency of these composites can be observed. Up to a nanoparticles concentration of 2 g/l could be embedded in the PDMS while keeping its transparency. Above this concentration the transparency decreased considerably (see for instance the image corresponding to the composite containing a nanoparticles concentration of 5 g/l). To verify that the nanoparticles were embedded uniformly in the polymer, we collected up-conversion emission maps of the composites (see Figure 4(b)), coupling the excitation and focusing parts of our setup to a CCD camera that substituted the digital color sensor. The images presented here are a composition of multiple images collected with this setup to show an enlarged area of the composites. As can be seen in these images, for concentrations above 2 g/l, the background luminescence of the composite dominates over the luminescence arising from the discrete nanoparticles, due to the high quantity of Ln-UCNPs that are excited at the same time by the diode laser, even if they are out of focus. This would affect the thermal measurement parameters of a device based on this material. Thus, composites containing a lower nanoparticles concentration will be used for further characterizations. An image of the luminescence that can be obtained in a Er,Yb:$NaYF_4$/PDMS composite with a concentration of 0.5 g/l is shown in Figure 4(c). In the image it can be appreciated the high transparency of the Er,Yb:$NaYF_4$/PDMS composite and the bright green luminescence that can be achieved after pumping at 980 nm with a power of 100mW. In the inset, the luminescence map corresponding to a cross-section of this composite is shown, indicating a similar dispersion degree of the UCNPs in the polymer than that observed in the top-view images. This would ensure accuracy enough for the determination of temperature by luminescence measurements using a microchip based on this composite.

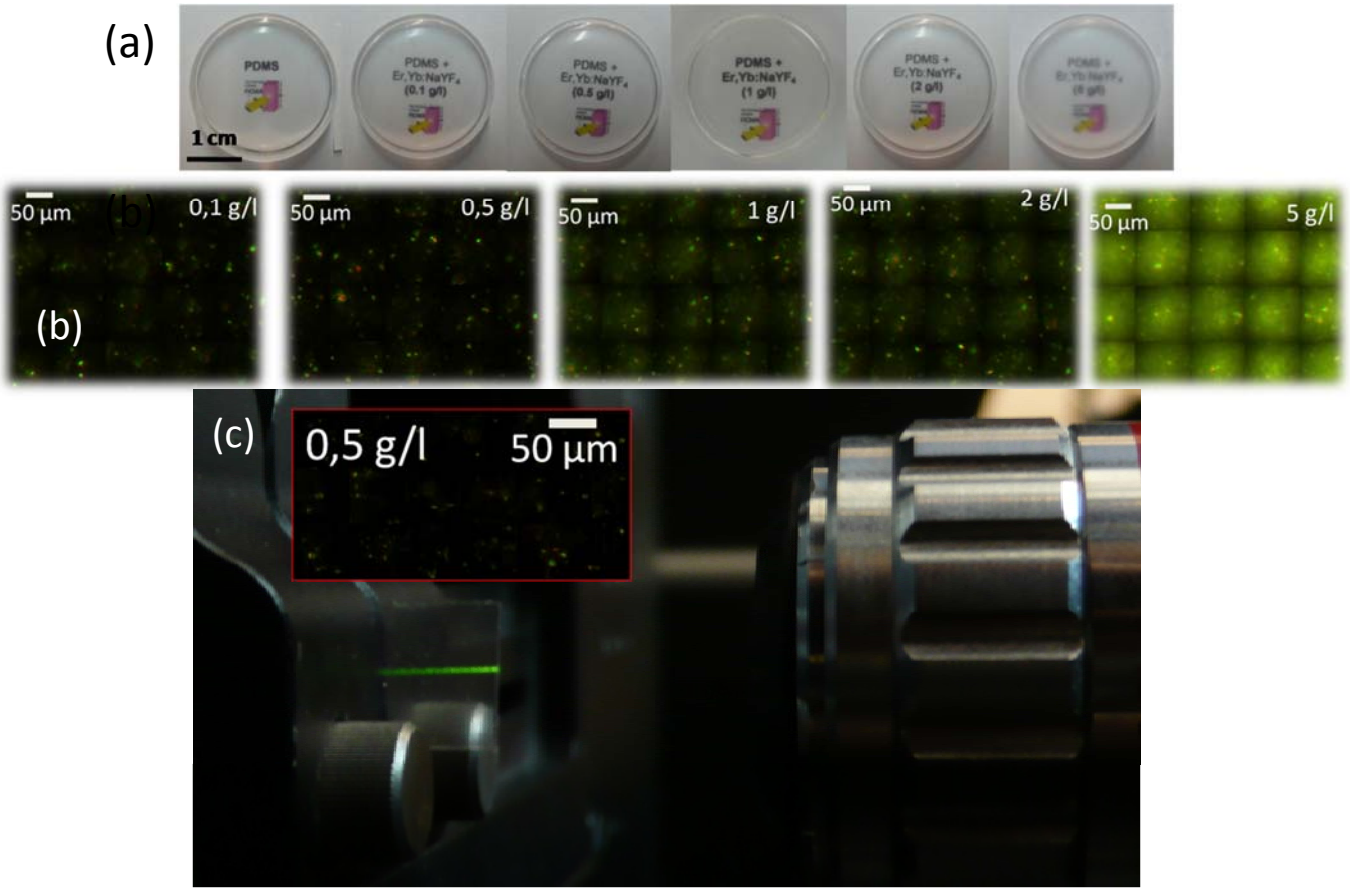

Figure 4. (a) Images of the Er,Yb:$NaYF_4$/PDMS composites containing different concentration of nanoparticles; (b) Up-conversion emission maps of selected composites; (c) Cross-section image of the 0,5 g/lEr,Yb:$NaYF_4$/PDMS composite showing the bright green emission that can be generated by the Er,Yb:$NaYF_4$ nanoparticles embedded in the polymer after pumping at 980 nm with a power of 100mW. The inset shows the corresponding luminescence map, indicating the homogeneity of the distribution of the nanoparticles.

To demonstrate the potential of these composites as luminescent thermometers we introduced a piece of them in a Linkam THMS 600 heating stage, to stabilize their temperature, and recorded their emission signals using the digital color sensor, from which we determined the RGB data ratio. Figure 5 (a) shows the temperature dependence of the intensity ratio corresponding to the signals recorded in the red and green channels of the digital color sensor for the Er,Yb:$NaYF_4$/PDMS composites with different concentrations of nanoparticles in the biological range of temperatures. The graph shows that for the samples containing a higher concentration of Ln-UCNPs the slope of these curves is smaller or even negative when the temperature increased, an effect that can be attributed to the background fluorescence arising from the nanoparticles which are out of focus, but that are still excited by the laser. The sample containing a particles concentration of 0.5 g/l shows an almost linear evolution of the red/green ratio. From its side, the sample containing 0.1 g/l of Ln-UCNPs shows an exponential increase of the red/green ratio as the temperature increased, following a tendency similar to that of the bare nanoparticles. Thus,

this sample would be the most appropriate to develop a microfluidic device in which we can monitor the temperature evolution in the whole chip, since it would provide the highest thermal sensitivity and thermal resolution. When we compare the relative thermal sensitivity of the 0.1 g/l Er,Yb:$NaYF_4$/PDMS composite with that of the bare nanoparticles (see Figure 5(b)), we observe that it is a little lower, maybe related to the interaction of light with the PDMS media [51], or the change of refractive index contrast between the two materials, but it is still similar to that reported in some publications for bare Er,Yb:$NaYF_4$ nanoparticles [20], indicating that we still can use this composite to determine the temperature by luminescence means.

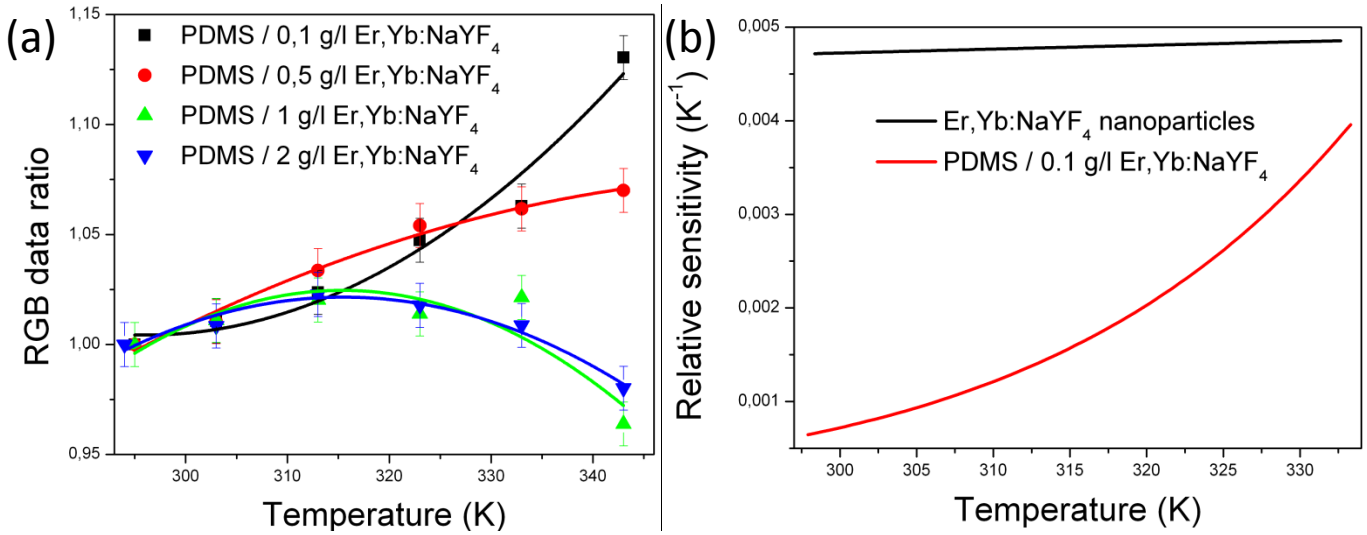

Figure 5. (a) RGB data ratio corresponding to different Er,Yb:$NaYF_4$/PDMS composites, containing different concentrations of Ln-UCNPs, as a function of temperature in the biological range. (b) Comparison of the relative thermal sensitivity of the 0.1 g/l Er,Yb:$NaYF_4$/PDMS composite and that of the bare Er,Yb:$NaYF_4$ nanoparticles.

4. Conclusions

We developed a new novel non-contact and non-invasive luminescence thermometer by using a commercial digital color sensor that allows collecting signals simultaneously in the blue, green and red channels of the electromagnetic spectrum, used usually to assess the quality of computer screens and used for the first time here to determine temperature from luminescence thermometry measurements, coupled to an excitation and an optical focusing system, together with luminescent up-conversion nanoparticles with emission in at least two of the detection channels of the digital color sensor. This detection setup simplifies substantially the design of other setups reported previously for the same purposes, and at the same time simplifies the alignment of the different optical components involved in the measurements (light sources, lenses, mirrors and detectors). Furthermore, it also simplifies the measurement procedures, while reduces the measurement and processing times of the luminescent signals to extract the temperature

of the sample analyzed. We demonstrated the potentiality of this setup for temperature sensing, by using Er,Yb:$NaYF_4$ nanoparticles emitting in the green and the red, with interest to explore temperatures in the biological range, and Tm,Yb:$GdVO_4$ nanoparticles emitting in the blue and the red, able to work up to 673 K, and thus, with interest in the microelectronic area to detect hot spots in microchips, for instance. The relative thermal sensitivity achieved with our setup is similar to that reported for the same kind of nanoparticles using conventional configurations in the fluorescence intensity ratio technique for temperature determination, which validates our new setup for temperature measurements. To improve the thermal resolution that can be achieved with this system two different strategies have been envisaged: (i) selecting luminescent nanoparticles with emissions that matches the maximum sensitivity of the detection channels of the digital sensor, and (ii) improving the luminescence collecting system, allowing the capture of a higher solid angle, for instance, so that we can have an intensity of emission in the range of optimal performance of the digital sensor. Furthermore, we have also shown that by embedding upconverting Er,Yb:$NaYF_4$ nanoparticles in PDMS, a standard polymer used for the fabrication of microfluidic devices useful for biomedical applications, we can generate composites that keep the transparency of PDMS and that might allow the fabrication of thermometric microfluidic chips, in which the same chip can be used as a luminescent thermometer for temperature determination in the walls of the microchannels.

Acknowledgements

This work was supported by the Spanish Government under Projects No. MAT2013-47395-C4-4-R, TEC2014-55948-R and MAT2014-56607-R, and by Catalan Authority under Project No. 2014SGR1358.Ol. A. Savchuk is supported by Catalan Government through the fellowship 2015FI_B2 00136. F. D. acknowledges additional support through the ICREA Academia awards 2010ICREA-02 for excellence in research.

References

[1] E. Carrasco, B. del Rosal, F. Sanz-Rodríguez, A. Juarranz de la Fuente, P. Haro Gonzalez, U. Rocha, K.U. Kumar, C. Jacinto, J. García Solé, D. Jaque, Intratumoral thermal reading during photo-thermal therapy by multifunctional fluorescent nanoparticles, Adv. Funct. Mater. 25 (2015) 615-626.

[2] J. L. Roti Roti, Cellular responses to hyperthermia (40-46 degrees C): cell killing and molecular events, Int. J. Hyperther. 24 (2008) 3–15.

[3] E.C. Ximendes, U. Rocha, C. Jacinto, K.U. Kumar, D. Bravo, F.J. López, E. Martín Rodríguez, J. García-Solé, D. Jaque, Self-monitored photothermal nanoparticles based on core-shell engineering, Nanoscale 8 (2016) 3057-3066.

[4] E.C. Ximendes, W.Q. Santos, U. Rocha, K.U. Kumar, F. Sanz-Rodríguez, N. Fernández, A. Gouveia-Neto, D. Bravo, A. Martín Domingo, B. del Rosal, C.D.S. Brites, L.D. Carlos, D. Jaque, C. Jacinto, Unveiling in vivo subcutaneous thermal dynamics by infrared luminescent nanothermometers, Nano Lett. 16 (2016) 1695-1703.

[5] M. P. Groover, Fundamentals of modern manufacturing: materials, processes and systems, fourth ed., John Wiley & Sons Inc., Hoboken, 2010.

[6] D. Jaque, F. Vetrone, Luminescence nanothermometry, Nanoscale 4 (2012) 4301–4326.

[7] C.D. Brites, P.P. Lima, N.J. Silva, A. Millan, V.S. Amaral, F. Palacio, L.D. Carlos, Thermometry at the nanoscale, Nanoscale 4 (2012) 4799–4829.

[8] M. Asheghi, Y. Yang, Micro- and nano-scale diagnostic techniques for thermometry and thermal imaging of microelectronic and data storage devices, in microscale diagnostic techniques, in: K. S. Breuer (ed.), Springer-Verlag, Berlin, 2005, pp. 155–196.

[9] J. Christofferson, K. Maize, Y. Ezzahri, J. Shabani, X. Wang, A. Shakouri, Microscale and nanoscale thermal characterization techniques, J. Electron. Packaging, 130 (2008) 041101–041106.

[10] A. H. Khalid, K. Kontis, Thermographic phosphors for high temperature measurements: principles, current state of the art and recent applications, Sensors 8 (2008) 5673–5744.

[11] P. Haro-González, L. Martínez-Maestro, I. R. Martín, J. García-Solé, D. Jaque, High-sensitivity fluorescence lifetime thermal sensing based on CdTe quantum dots, Small 8 (2012) 2652–2658.

[12] L.M. Maestro, E.M. Rodríguez, F.S. Rodríguez, M.C. Iglesias-de la Cruz, A. Juarranz, R. Naccache, F. Vetrone, D. Jaque, J.A. Capobianco, J. García Solé, CdSe quantum dots for two-photon fluorescence termal imaging, Nano Lett. 10 (2010) 5109–5115.

[13] P.A.S. Jorge, M.A. Martins, T. Trindade, J.L. Santos, F. Farahi, Optical fiber sensing using quantum dots, Sensors-Basel 7 (2007) 3489–3534.

[14] G. Walker, V. Sundar, C. Rudzinski, A. Wun, M. Bawendi, D. Nocera, Quantum-dot optical temperature probes, Appl. Phys. Lett. 83 (2003) 3555-3557.

[15] W. Jung, Y.W. Kim, D. Yim, J.Y. Yoo, Microscale surface thermometry using SU8/Rhodamine-B thin layer, Sens. Actuators A 171 (2011) 228–232.

[16] T. Barilero, T. Le Saux, C. Gosse, L. Jullien, Fluorescent thermometers for dual-emission-wavelength measurements: molecular engineering and application to thermal imaging in a microsystem, Anal. Chem. 81 (2009) 7988–8000.

[17] Y. Shiraishi, R. Miyarnoto, T. Hirai, A hemicyanine-conjugated copolymer as a highly sensitive fluorescent thermometer, Langmuir 24 (2008) 4273– 4279.

[18] E. Saïdi, B. Samson, L. Aigouy, S. Volz, P. Low, C. Bergaud, M. Mortier, Scanning thermal imaging by near-field fluorescence spectroscopy, Nanotechnology 20 (2009) 115703.

[19] S.K. Singh, K. Kumar, S.B. Rai, Er^{3+}/Yb^{3+} codoped Gd_2O_3 nano-phosphor for optical thermometry, Sens. Actuators A 149 (2009) 16–20.

[20] F. Vetrone, R. Naccache, A. Zamarron, A. J. de la Fuente, F. Sanz-Rodriguez, L. M. Maestro, E.M. Rodriguez, D. Jaque, J. García Sole, J.A. Capobianco, Temperature sensing using fluorescent nanothermometers, ACS Nano 4 (2010) 3254–3258.

[21] N.N. Dong, M. Pedroni, F. Piccinelli, G. Conti, A. Sbarbati, J.E. Ramirez-Hernandez, L.M. Maestro, M.C. Iglesias-de la Cruz, F. Sanz-Rodriguez, A. Juarranz, F. Chen, F. Vetrone, J.A. Capobianco, J. García Sole, M. Bettinelli, D. Jaque, A. Speghini, NIR-to-NIR two-photon excited

$CaF_2:Tm^{3+}$, Yb^{3+}nanoparticles: multifunctional nanoprobes for highly penetrating fluorescence bioimaging, ACS Nano5 (2011) 8665–8671.

[22] E. Navarro Cerón, D.H. Ortgies, B. del Rosal, F. Ren, A. Benayas, F. Vetrone, D. Ma, F. Sanz-Rodríguez, J. García Solé, D. Jaque, E. Martín Rodríguez, Hybrid nanostructures for high-sensitivity luminescence nanothermometry in the second biological window, Adv. Mater. 27 (2015) 4781-4787.

[23] Ol. A. Savchuk, J. J. Carvajal, J. Massons, M. Aguilo, F. Diaz, "Dispositivo y metodo para medida remota de temperature," Spain, P3110ES00, August 5, 2014.

[24] A.J. Downard, D.J. Garret, E.S.Q. Tan, Microscale patterning of organic films on carbon surfaces using electrochemistry and soft lithography, Langmuir 22 (2006) 10739-10746.

[25] J. Zhou, A.V. Ellis, N.H. Voelcker, Recent developments in PDMS surface modification for microfluidic devices, Electrophoresis 31 (2010) 2−16.

[26] L.J. Davis III, M. Deutsch, Surface plasmon based thermo-optic and temperature sensor for micro-fluidic thermometry, Rev. Sci. Instrum. 81 (2010) 114905.

[27] http://www.hamamatsu.com/resources/pdf/ssd/s9706_kpic1060e.pdf

[28] L.H. Fischer, G.S. Harms, O.S. Wolfbeis, Upconverting nanoparticles for nanoscale thermometry, Angew. Chem. Int. Ed. 50 (2011) 4546-4551.

[29] R. Calderon-Villajos, C.Zaldo, C. Cascales, Enhanced upconversion multicolor and white light luminescence in SiO_2-coated lanthanide-doped $GdVO_4$ hydrothermal nanocrystals, Nanothechnology 23 (2012) 505205.

[30] O.A. Savchuk, J.J. Carvajal, C. Cascales, J. Massons, M. Aguiló, F. Díaz, Thermochromic upconversion nanoparticles for visual temperature sensors with high thermal, spatial and temporal resolution, Nanoscale (submitted).

[31] M. Haase, H. Schäfer, Upconverting nanoparticles, Angew. Chem. Int. Ed. 50 (2011) 5808-5829.

[32] B. Dong, B. Cao, Y. He, Z. Liu, Z. Li, Z. Feng, Temperature sensing and in vivo imaging by molybdenum sensitized visible upconversion luminescence of rare-earth oxides, Adv. Mater. 24 (2012) 1987-1993.

[33] S. Zhou, K. Deng, X. Wei, G. Jiang, C. Duan, Y. Chen, M. Yin, Upconversion luminescence of $NaYF_4:Yb^{3+}$, Er^{3+} for temperature sensing, Optics Commun. 291 (2013) 138-142.

[34] Ol.A. Savchuk, P. Haro-Gonzalez, J.J. Carvajal, D. Jaque, J. Massons, M. Aguiló, F. Díaz, Er:Yb:NaY_2F_5O up-converting nanoparticles for sub-tissue fluorescence lifetime thermal sensing, Nanoscale 6 (2014) 9727-9733.

[35] S. Jiang, P. Zeng, L. Liao, S. Tian, H.Guo, Y. Chen, C. Duan, M. Yin, Optical thermometry based on upconverted luminescence in transparent glass ceramics containing $NaYF_4:Yb^{3+}/Er^{3+}$ nanocrystals, J. Alloys Comp. 617 (2014) 538–541.

[36] Z. Wang, D. Ananias, A. Carné-Sánchez, C.D.S. Brites, I. Imaz, D. Maspoch, J. Rocha, L.D. Carlos, Lanthanide-organic framework nanothermometers prepared by spray-drying, Adv. Funct. Mater. 25 (2015) 2824-2830.

[37] C. W. Shields IV, C. D. Reyes, G. P. Lopez, Microfuidic cell sorting: a review of the advances in the separation of cells from debulking to rare cell isolation, Lab Chip 15 (2015) 1230-1249.

[38] S. Köster, F. E. Angilè, H. Duan, J.J. Agresti, A. Wintner, C. Schmitz, A.C. Rowat, C.A. Merten, D. Pisignano, A.D. Griffiths, Drop-based microfluidic devices for encapsulation of single cells, Lab Chip 8 (2008) 1110-1115.

[39] F.M. Weinert, J.A. Kraus, T. Franosch, D. Braun, Microscale fluid flow induced by thermoviscous expansion along a traveling ware, Phys. Rev. Lett. 100(2008) 164501.

[40] M. U. Kopp, A. J. de Mello, A. Manz, Chemical amplification: continuous-flow PCR on a chip, Science 280 (1998) 1046-1048.
[41] P.R.N. Childs, J.R. Greenwood, C.A. Long, Review of temperature measurement, Rev. Sci. Instrum. 71 (2000) 2959-2978.
[42] L. J. Davis, M. Deutsch, Surface plasmon based thermo-optic and temperature sensor for microfluidic thermometry, Review of Sci Inst. 81(2010) 114905.
[43] K. L. K. Liu, K. L. Davis, M. D. Morris, Raman spectroscopic measurement of spatial and temporal temperature gradients in operating electrophoresis capillaries, Anal. Chem. 66 (1994) 3744-3750.
[44] M. E. Lacey, A. G. Webb, J. V.Sweedler, Monitoring temperature changes in capillary electrophoresis with nanoliter-volume NMR thermometry, Anal. Chem. 2000, 72, 4991-4998.
[45] N. Ishiwada, S. Fujioka, T. Ueda, T. Yokomori, Co-doped Y_2O_3:Tb^{3+} / Tm^{3+} multicolor emitting phosphors for thermometry, Opt. Lett. 36 (2011) 760-762.
[46] R.A. Mendels, E.M. Graham, S.W. Magennis, A.C. Jones, F. Mendels, Quantitative comparison of thermal and solutal transport in a T-mixer by FLIM and CFD, Microfluid. Nanofluid. 5 (2008) 603-617.
[47] X. Deng, B. Liu, S. Cao, R. Luo, H.Chen, A novel approach for the preparation of PMMA-PDMS core-shell particles with PDMS in the shell, Appl. Surf. Sci. 253 (2007) 4823−4829.
[48] M. George, R. G. Weiss, Molecular organogels. Soft matter comprised of low-molecular-mass organic gelators and organic liquids, Acc. Chem. Res. 39 (2006) 489−497.
[49] C. Fang, L. Shao, Y. Zhao, J. Wang, H. Wu. A gold nanocrystal/poly(dimethylsiloxane) composite for plasmonic heating on microfluidic chips, Adv. Mater. 24 (2012) 94-98.
[50] Y. Jiang, H. Wang, S. Li, W. Wen, Applications of micro/nanoparticles in microfluidic sensors: a review, Sensors 14 (2014) 6952-6964.
[51] H. Fu, G. Yang, S. Gai, N. Niu, F. He, J. Xu, P. Yang, Color-tunable and enhanced luminescence of well-defined sodium scandium fluoride nanocrystals, Dalton Trans. 42(2013) 7863-7870.

Oleksandr Savchuk is currently a PhD student at the Physics and Crystallography of Materials and Nanomaterials (FiCMA-FiCNA) research group of the Department of Physical Chemistry and Inorganics of the Universitat Rovira i Virgili, Tarragona (Spain). His research is focused on the developing new materials and new detection techniques for the luminescence nanothermometry.

Joan J. Carvajal is Vice-Dean of the Faculty of Chemistry, associate professor at the Department of Physical Chemistry and Inorganics of the Universitat Rovira i Virgili, and member of the Physics and Crystallography of Materials and Nanomaterials (FiCMA-FiCNA) research group, in Tarragona (Spain). He was awarded a PhD in Chemistry in 2003 from the Universitat Rovira i Virgili, and then joined the Department of Materials Science of the State University of New York at Stony Brook as a Fulbright post-doctoral research for two years. In 2006 he came back to the University Rovira i Virgili as a Ramon y Cajal post-doctoral researcher, and became associate professor in 2011. He is currently developing research in the fields of luminescence nanothermometry and porous GaN photonic sensors for early cancer detection and treatment.

Jaume Massons is an associate professor since 1990 at the Department of Physical Chemistry and Inorganics of the Universitat Rovira i Virgili in Tarragona, Spain. He is a member of the Physics and Crystallography of Materials and Nanomaterials (FiCMA-FiCNA) research group, where he collaborates in the development of the optical laboratory facilities. Currently, his research involves the application of opto-microfluidic techniques to bio-engineering problems, including sensing, quantification and micro-manipulation of cells using luminescent materials.

Concepción Cascales received the Ph.D. degree in solid-state chemistry from the University Complutense of Madrid, Madrid, Spain, 1986. After postdoctoral research at the Laboratoire de Chimie Métallurgique et Spectroscopie des Terres Rares, UPR 209 of the CNRS at Meudon-Bellevue, and at the École Nationale Supérieure de Chimie de París, ParisTech, France, she became a staff member of the Institute of Material Science of Madrid ICMM, Spanish Research Council CSIC. Presently, she is Research Professor at the Department of Photonic Materials at the ICMM. Her current research projects deal with the development of alternative image technologies based on NLO micro/nanomaterials, and bulk disordered crystals for femtosecond lasers.

Magdalena Aguiló received her BsC in Physics and her PhD in Physics in 1983 from the University of Barcelona, Barcelona, Spain. Currently, she is Full Professor of Crystallography at University Rovira i Virgili (URV), Tarragona, Spain. She received the *Professor Distingit* award by URV (2013).Her research interests include structural characterization of crystalline materials by X-ray diffraction and synchrotron, anisotropy of the physical properties of materials in relation with their crystalline structure, and crystal growth of bulk, epitaxial layers, nanoparticles and nanostructured materials.

Francesc Diaz earned his BSc in Physics and his PhD in Physics in 1982 at the University of Barcelona (UB). He is full Professor of Applied Physics at Universitat Rovira i Virgili (URV) since 1992 and leader of the research group of Physics and Crystallography of Materials (FiCMA). He was a visiting fellow at University of Toronto and State University of New York. He received the *Innovació Docent* award by URV (2004), the *Vicens Vives* award by *Generalitat de Catalunya* (2004), the *Professor Distingit* award by URV (2006), the *Excel·lència Docent* award by URV (2010) and the *Icrea Academia* award 2010 by *Generalitat de Catalunya*.The research interests of F. Diaz are currently focused in nanoparticles and nanostructured materials for integrated optics, and photonic devices from laser, non linear optics and photonic crystals.